

Polarimetric calibration strategy for long-duration imaging with a ground-based SAR

K. Morrison, G. Cookmartin, J.C. Bennett, S. Quegan, and A. Race

Abstract. The Ground-Based Synthetic Aperture Radar (GB-SAR) facility in the UK provides high-resolution, fully polarimetrically calibrated L- through X-band SAR imagery, principally of targets of remote sensing interest such as soils and vegetation. The facility consists of an indoor laboratory and a portable outdoor imaging system. Details of the polarimetric calibrations of both systems are discussed, with consideration given to the special requirements of field operation. Because of the need to mechanically scan the real antenna to build up a synthetic aperture, the SAR imaging process is significantly longer than its airborne and satellite counterparts. Some of the extended imaging schemes, such as those used in three-dimensional tomographic imaging and diurnal monitoring campaigns, can last from hours to days. However, calibration is normally only possible just prior to, and just after, imaging, leaving the data susceptible to nonlinear system sensitivity fluctuations during the imaging process itself. To address this problem, a novel scheme is discussed that utilizes the signal that arises from the imperfection in the rf isolation of the antenna head as a diagnostic to account for sensitivity fluctuations. Variations of several decibels were seen on a time scale of hours over an extended 2 day measurement. Excellent agreement was found with radar cross section (RCS) fluctuations retrieved from contemporaneous SAR imagery of reference trihedrals placed in the scene.

Résumé. La station terrestre RSO GB-SAR (« ground-based SAR ») du Royaume-Uni fournit des images haute résolution étalonnées polarimétriquement des bandes RSO L jusqu'à X, principalement de cibles d'intérêt pour la télédétection telles que les sols et la végétation. La station comporte un laboratoire intérieur et un système imageur portable extérieur. On discute des questions relatives à l'étalonnage polarimétrique des deux systèmes et l'on s'intéresse en particulier aux exigences spécifiques des opérations sur le terrain. À cause de la nécessité de balayer mécaniquement l'antenne réelle pour construire une antenne synthétique, le processus de formation de l'image RSO est significativement plus long que ses variantes aéroportées ou satellitaires. Certaines des procédures imageantes plus complexes telles que celles utilisées pour les images tomographiques en 3D et les campagnes de suivi diurne, peuvent s'étendre sur des heures et même des journées. Toutefois, l'étalonnage est généralement possible seulement juste avant ou juste après l'acquisition d'image, exposant les données aux aléas des fluctuations non linéaires de la sensibilité du système au cours du processus de formation de l'image lui-même. Pour pallier ce problème, on discute d'une procédure novatrice qui utilise le signal provenant de l'imperfection de l'isolation rf de la tête de l'antenne comme diagnostic témoignant des fluctuations de sensibilité. Des variations de plusieurs décibels ont été observées sur la base temporelle des heures au cours d'une mesure s'étendant sur deux jours. Une très bonne concordance a été observée par rapport aux fluctuations RCS extraites des images RSO acquises simultanément de trièdres de référence placés sur le terrain.

[Traduit par la Rédaction]

Introduction

The Ground-Based Synthetic Aperture Radar (GB-SAR) microwave measurement facility in the UK is used to investigate the microwave backscatter of vegetation and soils from L- through to X-band in support of airborne and satellite SAR platforms. The facility consists of an indoor laboratory and a novel portable outdoor system (Morrison et al., 2003; Bennett et al., 2000), which are shown in **Figure 1**. The former consists of a 6 m long \times 4 m wide \times 3 m high microwave anechoic chamber. The outdoor system is based around a trailer-mounted, 10 m hydraulic lift and a four-by-four all-terrain vehicle.

In airborne and satellite SAR imaging the synthetic aperture is built up by the rapid motion of the platform, with imaging times on the order of 1 s. In the ground-based case, however, the aperture is built up by the mechanical scanning of the antenna across a scanner frame, such that the imaging time scale is much longer. The scanner drive systems use high-performance,

compact motors and gearheads, suited to applications requiring both high dynamic response and smooth slow-speed operation, with the antenna head static at the time of each measurement. It is stepped across the scanner at intervals of $\sim\lambda/4$, where λ is the wavelength. At each position, the response of the target to a series of discrete frequencies stepped over a prescribed bandwidth is measured. The total measurement time is ~ 1 s per antenna position, such that a single full-aperture one-dimensional (1D) scan takes several minutes at X-band (less at lower frequencies, which require coarser sampling intervals).

Received 29 March 2004. Accepted 10 August 2004.

K. Morrison.¹ Department of Aerospace, Power and Sensors, University of Cranfield, Royal Military College of Science, Shrivenham, Swindon SN6 8LA, UK.

G. Cookmartin, J.C. Bennett, S. Quegan, and A. Race. Sheffield Centre for Earth Observation Science, University of Sheffield, Hounsfield Road, Sheffield S3 7RH, UK.

¹Corresponding author (e-mail: K.Morrison@cranfield.ac.uk).

Polarimetric scans are built up by repeat scans with the appropriate antennas switched in. There are instances, however, where the imaging process can be much longer, from hours to days. Examples are three-dimensional (3D) tomographic imaging with the indoor system that requires dense sampling over a two-dimensional (2D) aperture, or a sequence of time-lapsed images looking for diurnal variability in a scene (Morrison et al., 2001; Brown et al., 2003). Calibration of the system is carried out with reference to targets with well-characterized polarimetric responses. Because it requires physical resetting of the scanning system into a calibration geometry, however, calibration of the system is normally only performed immediately prior to, and on completion of, the entire imaging measurement process.

For lengthy scanning times, there is a likelihood of unwanted nonlinear changes in the system characteristics that are unable to be accounted for by reference to the two calibration measurements. This paper discusses the polarimetric calibration processes for the GB-SAR facility and describes a novel methodology that utilizes the signal that arises from the imperfection in the rf isolation of the antenna head as a diagnostic to account for nonlinear system sensitivity fluctuations during long-duration imaging.

Polarimetric calibration

The antenna head simulates a monostatic antenna and consists of a polarimetric cluster of four pyramidal horn antennas (Vtx, Vrx, Htx, Hrx), visible in **Figure 1**. The transmission lines can be switched to select antenna pairs to obtain the VV, VH, HH, and HV polarimetric responses. The rf signals are routed to and from the scanning head via coaxial cable through flexible chain-link trunking to provide smooth cable feed and minimize bend damage. In both the outdoor and indoor systems it is necessary to deploy the system from the imaging mode into the calibration geometry, such that calibration is normally only carried out before and after imaging. For the outdoor system it involves turning the hoist through 90° from its imaging geometry and dropping to half height (**Figure 2**). The antennas are positioned to look directly down onto the target, currently aligned using a plumb line. The use of calibration targets with broad angular radar cross section (RCS) patterns is advantageous because it alleviates the requirement for high directional alignment, which can be difficult to achieve in field conditions.

The choice of calibration procedure is influenced by our particular polarimetric system characteristics and the measurement application. Reference against point targets with well-characterized polarimetric responses allows for the calculation and correction of the distortion matrices of the receive and transmit circuits (Freeman, 1992). Barnes (1986) and Whitt et al. (1991) have provided calibration techniques that use three point targets with known scattering matrices. These techniques are very sensitive to target alignment, however, and require precise knowledge of the theoretical values of the scattering matrices. For those systems that have

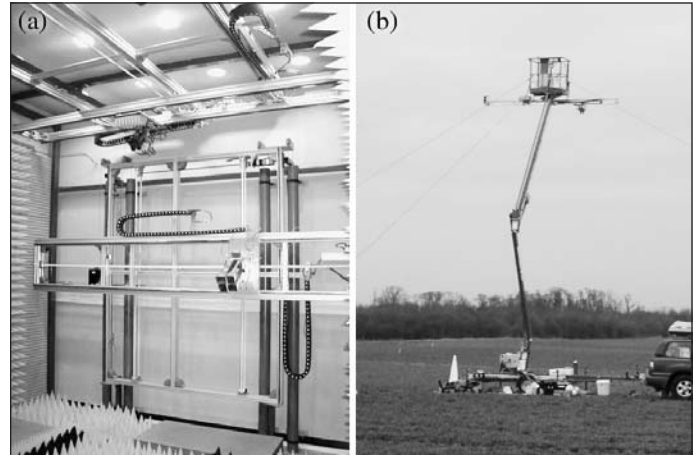


Figure 1. (a) View looking to one end of the anechoic chamber showing the 2.5 m × 3.7 m roof-mounted and 1.9 m × 3.7 m wall-mounted 2D scanners. The polarimetric antenna cluster is visible, as are the coaxial chain-link feeds. (b) The outdoor system deployed for imaging which scans the antenna head along a 4 m horizontal linear scanner.

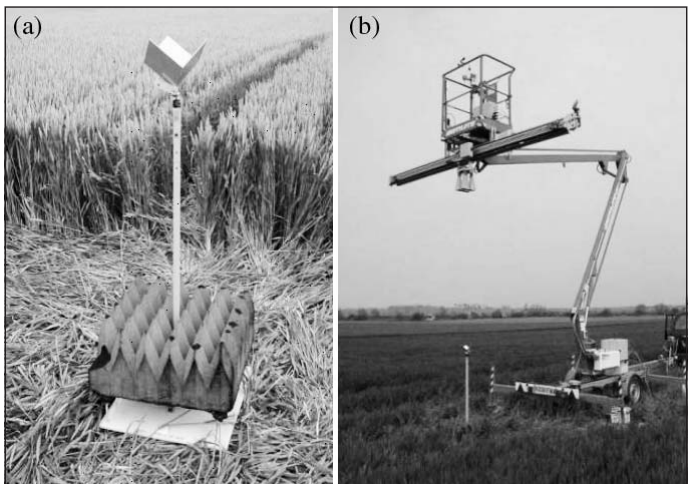


Figure 2. Calibration procedure for the outdoor system. (a) Calibration target. (b) The hoist has to be unguyed and moved through 90° from its imaging position shown in **Figure 1** and lowered into the calibration geometry with the antennas aligned looking directly down onto the calibration target shown in (a).

good crosstalk rejection, however, the method of Sarabandi et al. (1990) involves only two calibration targets. It removes the need to make a measurement of the crosstalk contamination, which is assumed to be zero. The GB-SAR system uses separate transmit and receive pyramidal horn antennas for both the indoor and outdoor systems. These antennas have low on-axis cross-polar response, and rejection is better than -30 dB across the bandwidth, such that we may reasonably approximate zero crosstalk.

With this procedure, only the co-polar target requires prior characterization, as the cross-polar scattering amplitude is described relative to the co-scattering amplitudes of the sphere and the ratio of the square root of the cross-polarized returns.

Use of a sphere, for which the scattering matrix can be computed exactly (Knott et al., 1993), and an arbitrary depolarizing target means that the procedure is robust to errors in orientation. Initially, a wire mesh held on a polystyrene tile was used as the unknown depolarizing target, but this was found to be difficult to control in windy conditions in field campaigns. It was replaced with a dihedral, which could be more easily held in position on the target support rod shown in **Figure 2**. The dihedral provides a controllable and continuously variable depolarized signal, which was sufficiently strong when the dihedral rotation was within $\sim 10^\circ$ of the maximum depolarizing 45° position (Chen et al., 1991). In addition, the dihedral backscatter response needs only to be aligned within its 3 dB width relative to the radar. The lack of accurate angular alignment requirements makes the method particularly attractive for GB-SAR field operations.

In the more controllable environment of the indoor chamber, a 6.4 cm diameter solid steel sphere is used as the precision co-polar target. A repeat measurement of a second, 5.0 cm sphere is made. The quality of the measured response of the first sphere is assessed by comparison with its predicted theoretical response and its ability to accurately predict the measured RCS of the second sphere. An example of a typical X-band calibration result for the 6.4 cm sphere is shown in **Figure 3**. The sphere is then replaced with an 8 cm \times 15 cm dihedral at 45° to measure the cross-polar response of the system.

Because the field equations involve the square root of a complex number, the calibration process can produce a phase ambiguity of 180° . To address this problem, in an extension to the method of Sarabandi et al. (1990), a second measurement of the dihedral is made, turned to 22.5° to provide equal co-polar and cross-polar returns. Because the phase relationship between the polarimetric returns is known for a dihedral (Chen et al., 1991), comparison with the measured phases resolves the ambiguity. For our extended version of this calibration, slightly more care needs to be taken to position the dihedral rotation angle to within $\sim 5^\circ$ and pointing direction within the 2 dB beam width. Such errors do not significantly affect the relative phase measured between the four polarization channels, allowing the ambiguity to be easily resolved.

The quality of the calibration is always assessed immediately, in case for any reason a repeat calibration measurement is required. Practical experience with GB-SAR has shown typical polarimetric calibration accuracy to be 0.2–1.0 dB in both the indoor and outdoor systems. Our measured dihedral results are interpreted in the image plane as complex RCS values so that they can be spatially segregated from other target responses. Taking typical values, we have found that the HV, VH, and one of the co-polar responses differ by less than 5° in phase, with the other co-polar response being out of phase by 180° to the same tolerance.

For the outdoor system, a slightly different calibration strategy is adopted. Because it operates in an environment with greater clutter, a sphere was found to be of insufficient RCS to provide a good enough signal-to-clutter ratio. Instead, a trihedral is used that has previously been calibrated against the

precision 6.4 cm sphere in the anechoic chamber and that provides a ~ 20 dB increase in signal. A trihedral has a broad beam pattern such that a sufficiently accurate angular alignment is easily achievable in field conditions. **Figure 4** compares the measured C-band VV and HH trihedral responses obtained during the outdoor calibration process with that measured in the indoor system. They are in good agreement, generally within ± 0.3 dB over the frequency bandwidth.

In addition to system effects, it is also necessary to account for the effects of the antenna beam pattern and processing gain in each polarization. Pyramidal horn antennas are used because they have well-prescribed beam patterns. This is particularly

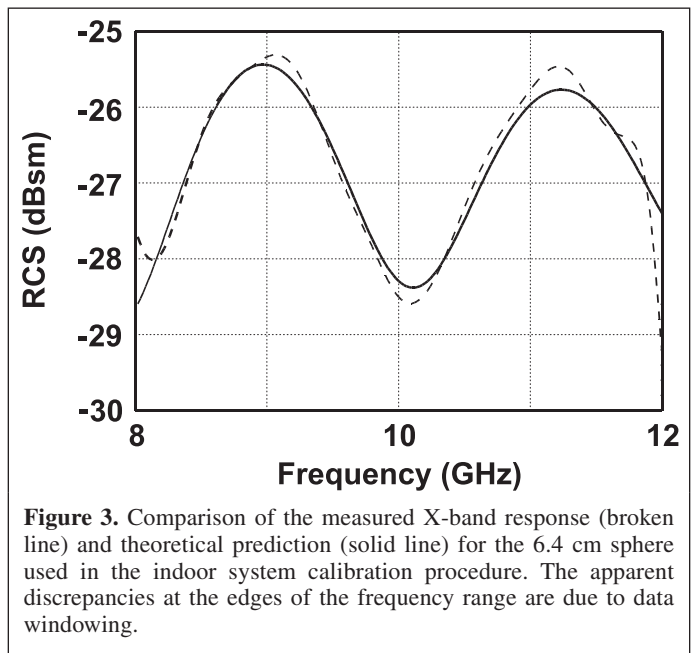


Figure 3. Comparison of the measured X-band response (broken line) and theoretical prediction (solid line) for the 6.4 cm sphere used in the indoor system calibration procedure. The apparent discrepancies at the edges of the frequency range are due to data windowing.

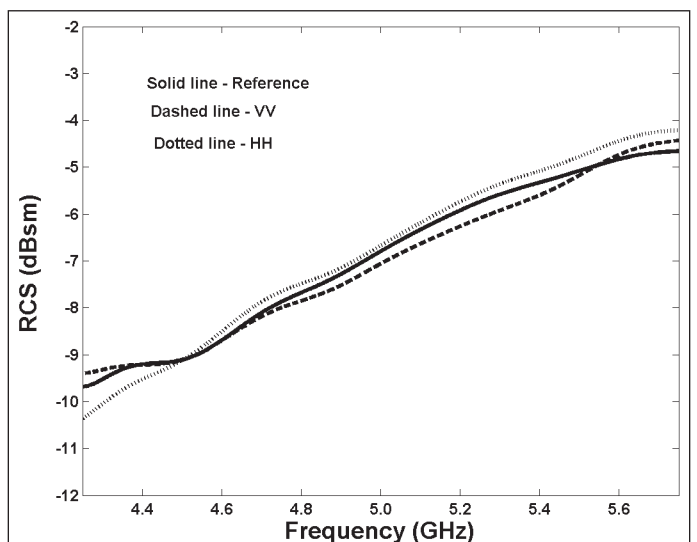


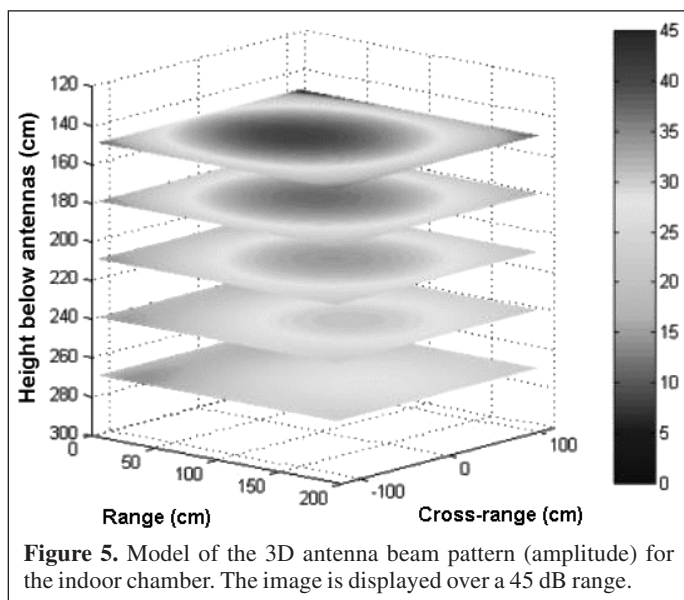
Figure 4. Comparison of the C-band VV (dashed line) and HH (dotted line) trihedral responses measured in an outdoor system calibration, plotted against the reference (solid line) trihedral response measured in the chamber. The VV/HH phase difference was constant to within $\pm 5^\circ$ across the bandwidth.

critical in the indoor system, where there can be a rapid change in beam pattern over and through the target owing to the proximity of the antenna and target. The correction is estimated using a full SAR simulation of the indoor and outdoor systems. **Figure 5** shows the 3D simulation of an antenna beam pattern over a 5 m^3 volume for the indoor system. This mode of presentation provides a more complete understanding of how the antenna beam pattern effects vary over the 3D target volume than a conventional 2D slice in angle representation. It is valuable for assessing the amplitude taper in any plane and is essential for estimating the usable imaging volume for a given configuration of SAR parameters.

The polarimetric calibration outlined here provides accurate calibration where the time span between the calibration and imaging measurements is short. In these cases, any drift between the two calibrations can be accounted for by a time-dependent linear adjustment over the imaging process. Where the imaging process is lengthy, however, there is the possibility of significant nonlinear fluctuation in the system response, which cannot be accounted for in the procedure outline here. In these cases a novel technique is outlined in the next section that provides constant monitoring of the system characteristics.

Correction for system drift

In some circumstances the duration of the imaging process can be lengthy, lasting from hours to days. It is normally only possible, however, to make a calibration measurement at the start and end of the imaging process. This has required the development of additional procedures that ensure confidence in the data from temporal system drifts and errors. Two independent calibration procedures are used to ensure self-consistency and confidence in the dataset. The external calibration procedure uses trihedrals placed in the scene as constant RCS references. The work reported here describes an



internal calibration procedure that makes novel use of the imperfection in the rf isolation of the antenna head.

In an ideal system, only the transmitted signal reflected from the target scene would enter the receive antenna; however, there is a coupled signal that leaks directly from the transmit antenna across to the receive antenna. This is normally regarded as an unwanted noise source, and steps are usually taken to minimize it. This coupling incorporates effects only from the vector network analyser (VNA), cables, amplifiers, and antennas, while excluding any propagation effects external to these. Examination of time-domain responses shows that typical target returns for the indoor system are only 3 dB below that of the coupled signal, and therefore both signals are well characterized after VNA digitization. The increased range of the outdoor system target means that target returns are typically 40 dB below the coupled signal, but this information is still stored with satisfactory accuracy within the 100 dB dynamic range of the digitizer.

Consideration of the nature of the coupled signal indicates that if there is no variation in the system parameters, the coupled signal should be spatially and temporally independent, i.e., of constant value throughout the measurement process. Any variation is therefore indicative of change in the response of the system. Phase information is readily available from the coupled signal and can be incorporated into the correction process. In this report, however, the observation program made it only necessary to retrieve properly corrected amplitude data.

In the measurement exercise, a series of image scans were made at 2 h intervals over a 44 h period with the outdoor system deployed as shown in **Figure 1**. The variation in the amplitude maximum of the coupled signal measured during and over a subset of four HH scans is shown in **Figure 6**. Each scan consists of 201 measurements along the aperture over a 5 min interval. To extract the coupled signal, it is spatially isolated at each aperture position by range gating following Fourier transformation of the frequency sweep to the time (range) domain.

Figure 6 shows a variation of 1.4 dB over the scan set selected. The in-scan variation is small, typically 0.1 dB, and in agreement with expected system performance. The principal feature is the offsets between scans due to system drift over the 6 h interval. To derive a value that might be applied to correct for the system drift in the HH data, a simple average of the maximum signal in each scan was calculated. Although one polarization is chosen here to demonstrate the method, leakage is present in all channels, and the principle of the technique applies equally well to all polarizations. The resulting development of the system response throughout the 44 h experiment, as monitored by the coupled signal, is shown in **Figure 7**. There is evidence of a diurnal cycle, with the maximum system response occurring at night and the minimum system response during the day. **Figure 8** shows the correlation of this same set of values with temperature, as measured by the weather station thermometer mounted on the GB-SAR hoist. The correlation is high but does not indicate a clear cause-and-effect relationship. It is still possible, however, that temperature

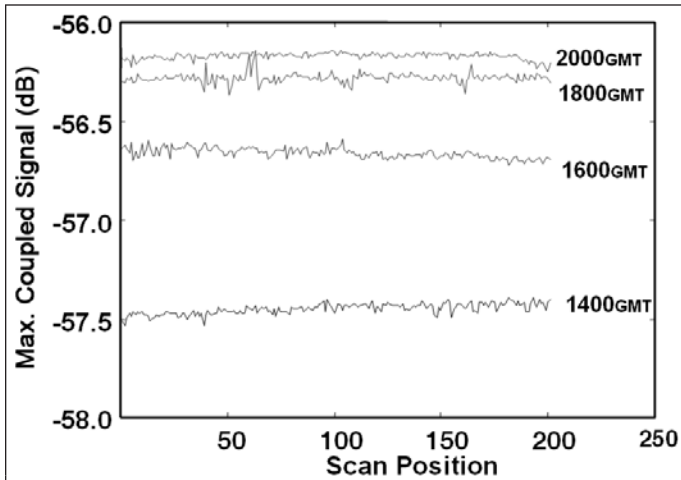


Figure 6. Temporal variation in the maximum amplitude of the coupled signal of the HH data over a 6 h period.

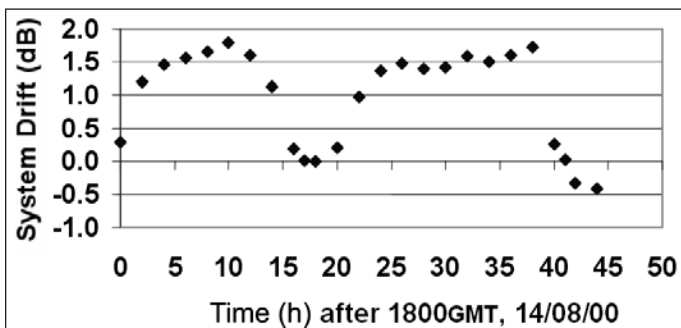


Figure 7. Averaged variation in the HH system response derived from the coupled signal over the entire 44 h measurement.

elsewhere in the system (e.g., inside the vehicle) is the governing influence on system response. There is no correlation with other environmental factors, such as wind-driven motion of the scanner arm (results not shown).

As is usual, two trihedrals were deployed at the far corners of the imaged scene. They provide fixed spatial reference points, and additionally a check on system stability. To show confidence in our interpretation of the variation measured by the coupled signal, **Figure 9** shows the HH system drift plotted against the variation in the trihedral RCS extracted from the corresponding SAR image. The correlation is very high, showing that the external and internal drift calibration methodologies provide consistent results.

The coupled signal also allows suspicious changes in system response to be picked up. The most likely problem is signal dropout associated with cable movement during the scanning process. Although a high-performance, lightweight Gore cable with a wire-wound core is used, fed to the antenna head through trunking well within the permitted bending radius, the continuous flexing and bending can lead to damage, such that the cables need to be regularly tested and replaced. The deterioration may lead to a general degradation in performance or produce sudden signal dropouts at certain points along the scan corresponding to particular cable positioning. As evidence

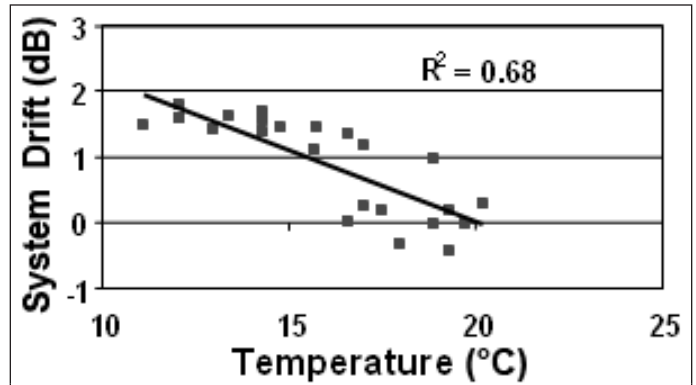


Figure 8. Correlation between the system drift, as measured by the coupled signal, and temperature recorded by the weather station at the top of the hoist.

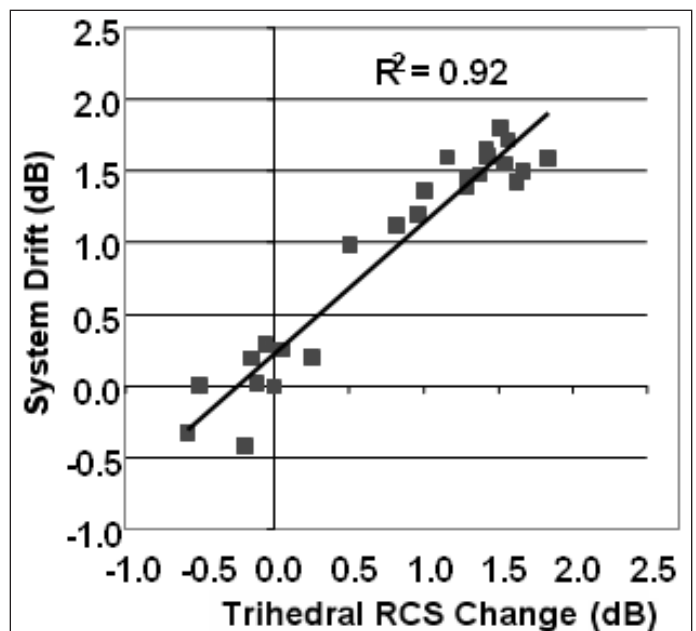


Figure 9. Correlation between the HH system drift as measured by the coupled signal and that measured by the variation in the RCS of a trihedral extracted from the sequence of SAR images.

of the use of the coupled signal as a diagnostic in system errors, **Figure 10** shows the near-contemporaneous VV dataset collected along with HH data displayed in **Figure 6**. In comparison, the VV scans show much larger variations, with a scan-to-scan variation of 2.8 dB. However, of principal concern are the large in-scan variations of up to 1.1 dB, well outside expected system performance. In this example, it was indicative of a fault in the VV circuit associated with the rf cable feed.

Summary

The polarimetric calibration strategy has been described for the GB-SAR facility. Co-polar and cross-polar responses are measured with references to a sphere and dihedral, respectively.

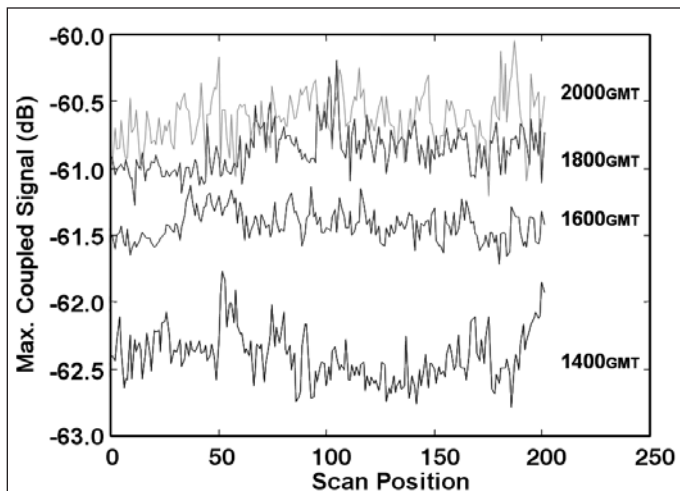


Figure 10. Temporal variation in the maximum amplitude of the coupled signal of the VV dataset over a 6 h period, collected near contemporaneous with the HH data shown in **Figure 6**.

In the more cluttered outdoor environment, a trihedral is used that has previously been calibrated against a sphere, to improve the signal-to-noise ratio. The use of targets with broad angular responses relaxes the need for accurate angular alignment, which is advantageous for fieldwork.

Operational logistics dictate that system calibration can only be carried out before and after imaging, but not during. Because the SAR imaging process can be lengthy, lasting from hours to days, there is the possibility of nonlinear temporal fluctuations in system sensitivity that cannot be accounted for by the two isolated calibrations. A procedure was demonstrated that can identify and correct for fluctuations during imaging. It utilizes the signal that arises from the imperfection in the rf isolation of the antenna head. Confirmation of the accuracy of the method was made by comparison with RCS fluctuations retrieved from contemporaneous SAR imagery of reference trihedrals.

Acknowledgements

The GB-SAR facility was built at the University of Sheffield using research grant F14/6/36 from the UK Natural Environment Research Council. The authors would like to thank Mr. D. Cox and Dr. A.J. MacDonald, and K.M. also wishes to thank the Department of Aerospace, Power and Sensors at the University of Cranfield.

References

Barnes, R.M. 1986. *Polarimetric calibration using in-scene reflectors*. Lincoln Laboratories, Massachusetts Institute of Technology, Lexington, Mass., Report TT.65.

Bennett, J.C., Morrison, K., Race, A.M., Cookmartin, G., and Quegan, S. 2000. The UK NERC fully portable polarimetric ground-based synthetic aperture radar (GB-SAR). In *IGARSS'00, Proceedings of the International Geoscience and Remote Sensing Symposium*, 24–28 July 2000, Honolulu, Hawaii. Edited by T.I. Stein. CD-ROM. IEEE, New York.

Brown, S.C.M., Quegan, S., Morrison, K., Bennett, J.C., and Cookmartin, G. 2003. High resolution measurements of scattering in wheat canopies — implications for crop retrieval. *IEEE Transactions on Geoscience and Remote Sensing*, Vol. 41, pp. 1602–1610.

Chen, T.-J., Chu, T.-H., and Chen, F.-C. 1991. A new calibration algorithm of wide band polarimetric measurement system. *IEEE Transactions on Antennas and Propagation*, Vol. 39, pp. 1188–1192.

Freeman, A.F. 1992. SAR calibration: an overview. *IEEE Transactions on Geoscience and Remote Sensing*, Vol. 30, pp. 1107–1121.

Knott, E.F., Shaeffer, J.F., and Tuley, M.T. 1993. *Radar cross section*. 2nd ed. Artech House, Inc., Norwood, Mass. Chapt. 5.

Morrison, K., Bennett, J.C., Cookmartin, G., McDonald, A.J., and Quegan, S. 2001. Three-dimensional X-band SAR imaging of a small conifer tree. *International Journal of Remote Sensing*, Vol. 22, pp. 705–710.

Morrison, K., Bennett, J.C., Cookmartin, G., Quegan, S., and Race, A. 2003. Development and capabilities of the ground-based SAR (GB-SAR) facility. In *Proceedings of the Advanced SAR Workshop*, 25–26 June 2003, Montréal, Que. CD-ROM. Canadian Space Agency, Saint-Hubert, Que.

Sarabandi, K., Ulaby, F.T., and Tassoudji, M.A. 1990. Calibration of polarimetric radar systems with good polarization isolation. *IEEE Transactions on Geoscience and Remote Sensing*, Vol. 28, pp. 70–75.

Whitt, M.W., Ulaby, F.T., Polatin, P., and Liepa, V.V. 1991. A general polarimetric radar calibration technique. *IEEE Transactions on Geoscience and Remote Sensing*, Vol. 39, pp. 62–67.